Memorias del XVI Congreso Latinoamericano
de Control Automático, CLCA 2014
Octubre 14-17, 2014. Cancún, Quintana Roo, México

Evaluation of Power Allocation in Wireless Networks under Multiplicative Noise and Interference Uncertainty ⋆

D.U. Campos-Delgado * **J.M. Luna-Rivera** * **A.J. Rojas** ** **C.A. Gutierrez** *

* *UASLP, Facultad de Ciencias, San Luis Potosi, Mexico, (e-mail: ducd@fciencias.uaslp.mx, mlr@fciencias.uaslp.mx, cagutierrez@fc.uaslp.mx).*
** *Universidad de Concepcion, Facultad de Ingenieria, Chile, (e-mail: arojasn@udec.cl).*

Abstract: In this paper, we study the problem of closed-loop power allocation in wireless networks subject to multiplicative interference and noise uncertainty. By using the mean-square small-gain theorem, stability bounds can be reached as a function of the size of the multiplicative uncertain terms: interference and noise. By establishing a numerical relation between the size of the interference and the multiplicative noise, a unique stability bound for power allocation is derived for a closed-loop structure. A numerical evaluation was carried out in a wireless network with multiple base stations and under different quality of service (QoS) requirements. Slow and fast-scale variations are considered in the channel model, as well as random displacements of the mobile units. In the evaluation, the power allocation scheme was able to achieve the desired QoS despite the multiple-access interference and multiplicative noise components.

Keywords: Power allocation, wireless network, small-gain, stochastic system.

1. INTRODUCTION

Nowadays wireless communications have reshaped people's lives by enabling remote, continuous and reliable information sharing despite geographical location. This idea has been possible by an elaborated physical networking, advanced signal processing tools, and powerful and low-cost hardware (Proakis and Salehi, 2007). Since more and more devices look to communicate wirelessly, this tendency creates a necessity to manage properly the increased interference induced by the wireless devices into the radio communication channels. Furthermore, the wireless transfer of information needs to satisfy certain quality-of-service (QoS) requirements, according to the required communication service: data, voice or video. For this purpose, several strategies have been proposed by the communications and signal processing communities: pre and post-equalization, beamforming, optimal signal detection, and power allocation (Campos-Delgado and Luna-Rivera, 2013-A), (Alpcan et al., 2008), (Gunnarsson and Gustafsson, 2003). In this sense, efficient utilization of the transmission power is fundamental, since this resource affects directly battery management. Hence, in the literature, there are have been proposals to regulate power allocation at the transmission stage by open and closed-loop schemes (Koskie and Z. Gajic, 2006). For example, there have been efforts focused on game theory and optimization approaches (Saraydar et al., 2002), linear-quadratic control (Campos-Delgado et al., 2010), H_∞ optimal control (Zhao et al., 2009), and switched PID structures (Safonov et al., 2005), among others. In fact, the first distributed power control proposal relied on a integral control with respect to the regulation error associated to the required QoS (Foschini and Miljanic, 1993). Meanwhile, due to the increased popularity of wireless sensor networks, power control has also been addressed in this context looking to reduce battery utilization (Messier et al., 2008).

In practical implementations, power allocation is carried out at discrete intervals with a fixed actualization rate (Lee, 2002), and under a limited word-length for feedback (Fazel and Kaiser, 2008). For this reason, the problem of quantization inside a discrete-time closed-loop strategy arises naturally (Su et al., 2011), (Fu and Xie, 2005). There have been a few works that addressed this issue in the context of power allocation for wireless systems, and mainly under a uniform quantization scheme (Campos-Delgado and Luna-Rivera, 2013-C), (Quevedo and Wigren, 2012). Nonetheless, in practice, the quantization process of the feedback information can have logarithmic or non-uniform patterns and floating-point representations (Lu and Skelton, 2000), resulting in multiplicative stochastic models to characterize the induced uncertainty in the feedback systems. Closed-loop control under a multiplicative noise component has been studied in (Lu and Skelton, 2000), (Lu and Skelton, 2002), by considering a robust control perspective. In this sense, our early work in Campos-Delgado et al. (2014) analyses theoretically for the first time this issue in the scene of power allocation for wireless networks. Hence, this work extends our previous contribution by a further evaluation of the stability bounds derived for the

⋆ This research was supported by grants from CONACYT (Refs. # 83811 and # 128976).

uncertain terms in the feedback path, and a comprehensive performance evaluation in a wireless network model subject to multiple base stations, multi-access environment, and slow and fast-scale channel variations.

The notation used in this paper is described next. $\mathbb{R}$ denotes the set of real numbers, and $\mathbb{R}^N$ represents real N-dimensional vectors. Scalars are represented by lowercase italic letters, and vector and matrices by boldface letters. $(\cdot)^\top$, $(\cdot)^H$ and $\text{Tr}(\cdot)$ describe the transpose, complex conjugate-transpose and trace operators, respectively. Meanwhile, $\mathbf{I}$ denotes the identity matrix, and $\lambda_{max}(\cdot)$ the maximum eigenvalue of a matrix. For complex vectors $\mathbf{x} = [x_1 \ \ldots x_N]^\top$, its Euclidean norm is expressed as $\|\mathbf{x}\| = \mathbf{x}^H\mathbf{x} = \sqrt{\sum_i |x_i|^2}$, and $\mathcal{E}\{\cdot\}$ represents the expectation operator of a random variable. For a one-sided discrete-time signal $f[k]$, its Z-transform is defined by $F(z) = \mathcal{Z}\{f[k]\}$. The $\mathcal{L}_2$ norm of a transfer matrix $\mathbf{T}(z)$ is represented by

$$\|\mathbf{T}(z)\|_2^2 = \frac{1}{2\pi}\int_{-\pi}^{\pi} \text{Tr}\left[\mathbf{T}^H(e^{j\omega})\mathbf{T}(e^{j\omega})\right] d\omega. \qquad (1)$$

For a discrete-time stochastic process $\mathbf{z}[k]$ valid for $k \geq 0$ with finite variance, its signal norm is defined by $\|\mathbf{z}\|_v^2 = \lim_{k\to\infty} \mathcal{E}\{\|\mathbf{z}[k]\|^2\}$. For a mapping from the signal space of finite variance stochastic processes into itself $\mathcal{T}$ with $\mathbf{z}[k] = \mathcal{T}(\mathbf{v}[k])$, its system norm is defined by

$$\|\mathcal{T}\|_s = \max_{\|\mathbf{v}\|_v \neq 0} \frac{\|\mathbf{z}\|_v}{\|\mathbf{v}\|_v} \qquad (2)$$

2. PROBLEM FORMULATION

In this work, we consider a general wireless communication network subject to multiple-access interference from the mobile units (MUs), as shown in Fig. 1. The active users could be in a mobile environment or at a fixed location, where each user sends its information to the nearest base station (BS). In the network, there are M BSs with $\mathcal{I}$ as the set of indexes associated to the MUs. The number of MUs U is then equal to the cardinality of $\mathcal{I}$, i.e. $\text{card}(\mathcal{I}) = U$. Due to its relation to battery management, the uplink path (BS to MUs) is addressed in this study, where the transmission power is adjusted iteratively in order to overcome the multiple-access environment and satisfy a desired QoS in the received information. The multiple-access scenario could be the result from the communication links of the active users from the same cell, such as in the case of CDMA or MC-CDMA technologies (Campos-Delgado and Luna-Rivera, 2013-A), or from neighbourhood cells by frequency re-use in OFDMA technology (Proakis and Salehi, 2007). The QoS in the network will be evaluated by the BER or FSR (Saraydar et al., 2002), which can be linked to the signal to interference-noise ratio (SINR) after signal detection if the channel-state information (CSI) is known. Therefore, if a linear detector is employed at the reception stage of the BS, the SINR for i-th user at k-time instant can be expressed as (Campos-Delgado and Luna-Rivera, 2013-A):

$$\gamma_i[k] = \frac{\delta_{i,i}[k]p_i[k]}{\sum_{l\in\mathcal{I}\setminus\{i\}} \delta_{i,l}[k]p_l[k] + \omega_i[k]} \qquad \forall i \in \mathcal{I} \qquad (3)$$

where $p_l[k]$ is the transmission power of l-th user, the term $\delta_{i,i}[k] > 0$ is related to the data energy of i-th active user, $\delta_{i,l}[k] \geq 0$ with $l \in \mathcal{I}\setminus\{i\}$ are values associated to the induced multiple-access interference to i-th active user by the l-th one, and $\omega_i[k]$ is the resulting noise energy.

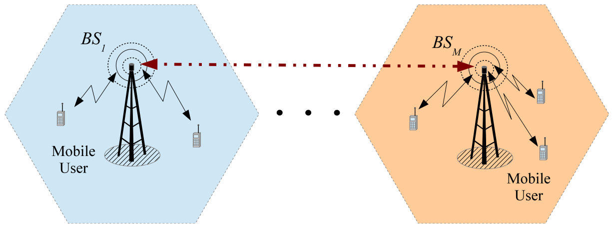

Fig. 1. Diagram of the Wireless Network Under Study.

3. UPLINK POWER CONTROL

The general power control framework in Campos-Delgado et al. (2010) is followed in this work. In this strategy, the first step is to quantify the error between the measured $\gamma_i[k]$ and objective SINRs γ_i^{obj} by using a percentage error in order to cancel the nonlinear pattern in the SINR metric:

$$e_i[k] = \left[\frac{\gamma_i^{obj} - \gamma_i[k]}{\gamma_i[k]}\right] p_i[k] = \left[\frac{\gamma_i^{obj}}{\gamma_i[k]} - 1\right] p_i[k] \quad \forall i \in \mathcal{I} \qquad (4)$$

where by a direct substitution of (3), an equivalent linear error description is obtained that can be written in vector notation $\mathbf{e}[k] = [e_1[k] \ \ldots \ e_U[k]]^\top$ as

$$\mathbf{e}[k] = (\mathbf{\Theta}[k] - \mathbf{I})\,\mathbf{p}[k] + \mathbf{d}[k] \qquad (5)$$

where $\mathbf{p}[k] = [p_1[k] \ \ldots \ p_U[k]]^\top$ is the transmission power vector, $\mathbf{\Theta}[k] \in \mathbb{R}^{U\times U}$ is a coupling matrix in the wireless network due to multiple-access interference, and $\mathbf{d}[k] = [d_1[k] \ \ldots \ d_U[k]]^T \in \mathbb{R}^U$ represents an external input term for the closed-loop system:

$$\mathbf{\Theta}[k] = \begin{bmatrix} 0 & \gamma_1^{obj}\frac{\delta_{1,2}[k]}{\delta_{1,1}[k]} & \cdots & \gamma_1^{obj}\frac{\delta_{1,U}[k]}{\delta_{1,1}[k]} \\ \gamma_2^{obj}\frac{\delta_{2,1}[k]}{\delta_{2,2}[k]} & 0 & \cdots & \gamma_2^{obj}\frac{\delta_{2,U}[k]}{\delta_{2,2}[k]} \\ \vdots & \vdots & \ddots & \vdots \\ \gamma_U^{obj}\frac{\delta_{U,1}[k]}{\delta_{U,U}[k]} & \gamma_U^{obj}\frac{\delta_{U,2}[k]}{\delta_{U,U}[k]} & \cdots & 0 \end{bmatrix} \qquad (6)$$

$$\mathbf{d}[k] = \left[\gamma_1^{obj}\frac{\omega_1[k]}{\delta_{1,1}[k]} \ \cdots \ \gamma_U^{obj}\frac{\omega_U[k]}{\delta_{U,U}[k]}\right]^\top. \qquad (7)$$

In our formulation, due to the statistical properties of the interference terms, the second order statistic of the coupling matrix $\mathbf{\Theta}[k]$ is assumed time-invariant

$$\Upsilon \triangleq \mathcal{E}\{\mathbf{\Theta}^\top[k]\mathbf{\Theta}[k]\} \quad \forall k \geq 0, \qquad (8)$$

where this consideration is consistent with a flat-fading channel profile (Proakis and Salehi, 2007). In this way, the error vector $\mathbf{e}[k]$ is a linear function of the power vector $\mathbf{p}[k]$ after the nonlinear transformation in (4) with a multiplicative component $\mathbf{\Theta}[k]$ related to the interference in the wireless network. During a real-time implementation, there are transport delays associated with the synchronization scheme in the BSs and SINR quantification process (Gunnarsson and Gustafsson, 2001), and to address this issue, n_{RT} represents the round-trip delay in the feedback systems. Therefore, if $\mathbf{a}[k] = [a_1[k] \ \ldots \ a_U[k]]^T$ denotes the received error vector from the BSs by the MUs at k-time instant, then this vector is modelled as

$$\mathbf{a}[k] \triangleq \mathbf{m}[k - n_{RT}]. \quad (9)$$

This discrete-time feedback process involves errors due to a finite wordlength related to the quantization process of the error signal (Su et al., 2011), and also to floating point operations in the computation of the tracking error. By considering a vector notation, the effect of the multiplicative noise can be written by a linear operator:

$$\mathbf{m}[k] = (\mathbf{I} + \mathbf{\Xi}[k])\,\mathbf{e}[k] \quad (10)$$

where

$$\mathbf{\Xi}[k] = \begin{bmatrix} \xi_1[k] & & \\ & \ddots & \\ & & \xi_U[k] \end{bmatrix}, \; \mathbf{m}[k] = \begin{bmatrix} m_1[k] \\ \vdots \\ m_U[k] \end{bmatrix}. \quad (11)$$

The terms $\xi_i[k]$ are random variables with a uniform distribution in the interval $[-\pi_i, \pi_i]$ for $\pi_i > 0$, where there is statistical independence between the multiplicative noise components and the tracking errors. The control problem is then formulated as the design of a distributed control strategy for the transmission power $p_i[k]$ for $i \in \mathcal{I}$ at k-time instant such that the SINR $\gamma_i[k]$ can reach an objective value $\gamma_i^{obj} > 0$, despite the effect of multiplicative noise components and multiple-access interference.

By using a $\mathcal{Z}$-Transform notation and at each MU, a linear power assignment rule is assumed:

$$p_i(z) = C_i(z)\, a_i(z) \qquad \forall i \in \mathcal{I} \quad (12)$$

where $C_i(z)$ denotes the controller for i-th MU, $p_i(z) = \mathcal{Z}\{p_i[k]\}$ and $a_i(z) = \mathcal{Z}\{a_i[k]\}$. Hence from (5), (9), (10) and (12), the overall dynamics in the wireless network can be established and they are graphically depicted in Fig. 2. As a result, in the closed-loop interaction inside the wireless network (see Fig. 2), there are two multiplicative uncertainty terms that could affect the internal stability of the distributed feedback loops: the multiple-access interference $\mathbf{\Theta}[k]$ in the network, and the random noise $\mathbf{\Xi}[k]$ due to non-uniform quantization and floating-point operations.

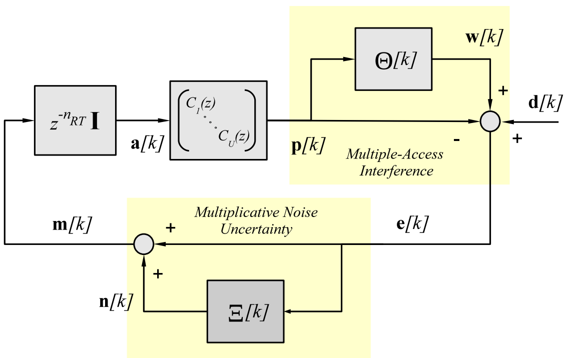

Fig. 2. Overall Closed-Loop Structure for Power Allocation.

4. CLOSED-LOOP ANALYSIS

In this section for the sake of completeness, we recall the results reported by Campos-Delgado et al. (2014) related to the internal stability of the closed-loop interaction in Fig. 2. First, the system norms of the two stochastic operators $\mathbf{\Theta}[k]$ and $\mathbf{\Xi}[k]$ are evaluated by considering that they represent static mappings with random parameters. Therefore, by the definition in (2), it is obtained:

$$\|\mathbf{\Theta}\|_s = \sqrt{\lambda_{max}(\Upsilon)} \quad (13)$$

$$\|\mathbf{\Xi}\|_s = \max_{i \in \mathcal{I}} \sigma_i, \quad (14)$$

where $\sigma_i^2 = \mathcal{E}\{\xi_i^2[k]\}$ for all $i \in \mathcal{I}$. Based on the mean-square small-gain theorem (Lu and Skelton, 2002), the next propositions establish two upper-bounds for internal stability, which are functions of the norms of the multiplicative uncertainty terms, and complementary sensitivity $T_i(z)$ and sensitivity $S_i(z)$ transfer functions of each distributed closed-loop system. Due to the distributed control structure, the global transfer functions are $\mathbf{T}(z) = \mathrm{diag}\{T_1(z), \ldots, T_U(z)\}$ and $\mathbf{S}(z) = \mathrm{diag}\{S_1(z), \ldots, S_U(z)\}$.

Proposition 1: The closed-loop system in Fig. 2 is robust stable if the multiplicative uncertainty terms satisfy

$$\|\mathbf{\Theta}\|_s^2 \times \|\mathbf{\Xi}\|_s^2 < \frac{1}{\|\mathbf{T}(z)\|_2^2 \left| \|\mathbf{T}(z)\|_2^2 - \|\mathbf{S}(z)\|_2^2 \right|} \quad (15)$$

$$\|\mathbf{\Theta}\|_s^2 + \|\mathbf{\Theta}\|_s^2 \cdot \|\mathbf{\Xi}\|_s^2 \left(\|\mathbf{T}(z)\|_2^2 - \|\mathbf{S}(z)\|_2^2 \right) + \|\mathbf{\Xi}\|_s^2 < \frac{1}{\|\mathbf{T}(z)\|_2^2}.$$

In the previous result, it is considered that the linear distributed controllers $C_i(z)$ are known a priori. To illustrate this idea, the LQG control derived in Campos-Delgado et al. (2010) which takes into account the round-trip delay n_{RT} and has important robustness properties is addressed in this work. This controller includes integral action and is expressed by

$$C_i(z) = \frac{\Omega}{1 - (1 - \Omega)z^{-1} - \Omega z^{-n_{RT}}} \qquad \forall i \in \mathcal{I}, \quad (16)$$

where the control gain is restricted $\Omega \in (0, 1)$ in order to guarantee closed-loop stability. Another important property of the LQG controller in (16) is that the internal stability conditions in (15) can be simplified by the exact computation of the $\mathcal{L}_2$ norms of the complementary sensitivity and sensitivity transfer functions, since $\|T_i(z)\|_2^2 = \Omega/(2-\Omega)$ and $\|S_i(z)\|_2^2 = 2/(2-\Omega)$ (Campos-Delgado and Luna-Rivera, 2013-C).

Proposition 2: Assume that the LQG controller in (16) is adopted by all the active users in the wireless network with the same control gain $\Omega \in (0, 1)$, then the closed-loop system in Fig. 2 is robust stable if the multiplicative uncertainty terms satisfy

$$\|\mathbf{\Theta}\|_s^2 \times \|\mathbf{\Xi}\|_s^2 < \frac{2 - \Omega}{U^2 \Omega} \quad (17)$$

$$\|\mathbf{\Theta}\|_s^2 + \|\mathbf{\Xi}\|_s^2 < \frac{2(2 - \Omega)}{U \Omega}. \quad (18)$$

5. ROBUST CONTROL ANALYSIS

In this section, we further analyze the upper bounds derived in Propositions 1 and 2 for robust stability. First, in discrete-time, we have that as long as $T_i(z) + S_i(z) = 1$ then $\|S_i(z)\|_2^2 = 1 + \|T_i(z)\|_2^2$, and thus in general $\left|\|\mathbf{T}(z)\|_2^2 - \|\mathbf{S}(z)\|_2^2\right| = U$. As a result, the inequalities in (15) are equivalent to

$$\|\mathbf{\Theta}\|_s^2 \times \|\mathbf{\Xi}\|_s^2 < \frac{1}{\|\mathbf{T}(z)\|_2^2 U}, \quad \|\mathbf{\Theta}\|_s^2 + \|\mathbf{\Xi}\|_s^2 < \frac{2}{\|\mathbf{T}(z)\|_2^2}.$$

Assume now that $\|\boldsymbol{\Xi}\|_s^2 = \alpha\|\boldsymbol{\Theta}\|_s^2$ with $\alpha > 0$, then we have

$$\|\boldsymbol{\Theta}\|_s^2 < \frac{1}{\|\mathbf{T}(z)\|_2\sqrt{\alpha U}} \triangleq B_1, \quad (19)$$

$$\|\boldsymbol{\Theta}\|_s^2 < \frac{2}{(1+\alpha)\|\mathbf{T}(z)\|_2^2} \triangleq B_2. \quad (20)$$

Remark: In Proposition 2, we have already implicitly assumed the knowledge of $\|\boldsymbol{\Theta}\|_s^2$ and $\|\boldsymbol{\Xi}\|_s^2$ for the tuning of the control gain Ω, in order to ensure robust stability. It is then always possible, with such knowledge, to quantify the value α that relates $\|\boldsymbol{\Xi}\|_s^2$ to $\|\boldsymbol{\Theta}\|_s^2$. We argue, in the rest of this section, that the introduction of α allows for an analysis that gives further insight into the requirements for robust stability when Ω is fixed and known.

The main question this section attempts to answer is which bound, B_1 or B_2, is the most stringent? To answer this, we consider the question in term of inequalities

$$\frac{1}{\|\mathbf{T}(z)\|_2\sqrt{\alpha U}} \leqslant \frac{2}{(1+\alpha)\|\mathbf{T}(z)\|_2^2}, \quad (21)$$

$$\Rightarrow \frac{1}{\sqrt{\alpha U}} \leqslant \frac{2}{(1+\alpha)\|\mathbf{T}(z)\|_2}. \quad (22)$$

The last step does not alter the possible inequality direction since by definition $\|\mathbf{T}(z)\|_2 > 0$. This previous inequality is equivalent to

$$0 \leqslant \frac{2}{(1+\alpha)\|\mathbf{T}(z)\|_2} - \frac{1}{\sqrt{\alpha U}} = \frac{2\sqrt{\alpha U} - (1+\alpha)\|\mathbf{T}(z)\|_2}{\sqrt{\alpha U}(1+\alpha)\|\mathbf{T}(z)\|_2}.$$

We observe that the denominator on the right-hand side is always positive (since U, α and $\|\mathbf{T}(z)\|_2^2$ are all positive), thus the condition becomes

$$0 \leqslant 2\sqrt{\alpha U} - (1+\alpha)\|\mathbf{T}(z)\|_2 \quad (23)$$

$$\Rightarrow \frac{1+\alpha}{\sqrt{\alpha}} \leqslant \frac{2\sqrt{U}}{\|\mathbf{T}(z)\|_2}. \quad (24)$$

Since by construction $\mathbf{T}(z)$ is a diagonal matrix with elements $T_i(z)$ $\forall i \in \mathcal{I}$, if we impose (as in the present work) that all these elements are equal, then we have

$$\frac{1+\alpha}{\sqrt{\alpha}} \leqslant \frac{2\sqrt{U}}{\sqrt{U}\|T_i(z)\|_2} \quad (25)$$

$$\therefore \frac{1}{\sqrt{\alpha}} + \sqrt{\alpha} \leqslant \frac{2}{\|T_i(z)\|_2}, \quad (26)$$

and consequently, the resulting condition is not a function of the number MUs U in the network. Therefore, we have a condition on α that determines which bound is the more stringent, that is if α satisfies

$$\frac{1}{\sqrt{\alpha}} + \sqrt{\alpha} > \frac{2}{\|T_i(z)\|_2} \Rightarrow B_1 > B_2, \quad (27)$$

and B_2 is the lowest bound, and thus the more stringent robust stability requirement. On the other hand, if α is such that

$$\frac{1}{\sqrt{\alpha}} + \sqrt{\alpha} < \frac{2}{\|T_i(z)\|_2} \Rightarrow B_1 < B_2, \quad (28)$$

and B_1 is the lowest bound, and thus the more stringent robust stability requirement. We now recall $\|T_i(z)\| = \Omega/(2-\Omega)$, and we have that

$$\frac{1}{\sqrt{\alpha}} + \sqrt{\alpha} \lessgtr 2\sqrt{\frac{2-\Omega}{\Omega}}. \quad (29)$$

As an example consider $\Omega = 0.6$ and two cases for the variable $\alpha \in \{\alpha_1, \alpha_2\}$ with $\alpha_1 = 2$ and $\alpha_2 = 10$. For α_1, we have that $1/\sqrt{\alpha_1} + \sqrt{\alpha_1} = 2.1213$, and thus this value is lower than $2\sqrt{(2-\Omega)/\Omega} = 3.0551$. As a result, we have that

$$B_1 = \frac{1}{U}\sqrt{\frac{2-\Omega}{\alpha\Omega}} = \frac{1.0801}{U} < \frac{1.5556}{U} = \frac{1}{U}\frac{2(2-\Omega)}{(1+\alpha)\Omega} = B_2,$$

and B_1 is effectively the more stringent bound, independent of the number of active users U. On the other hand, for $\alpha_2 = 10$, we have that $1/\sqrt{\alpha_2} + \sqrt{\alpha_2} = 3.4785$, and thus this value is greater than $2\sqrt{(2-\Omega)/\Omega} = 3.0551$. As a result, we have that

$$B_1 = \frac{1}{U}\sqrt{\frac{2-\Omega}{\alpha\Omega}} = \frac{0.4830}{U} > \frac{0.4242}{U} = \frac{1}{U}\frac{2(2-\Omega)}{(1+\alpha)\Omega} = B_2,$$

and B_2 is now effectively the more stringent bound.

In conclusion, both Propositions 1 and 2 present two sets of inequalities that need to be satisfied simultaneously for robust stability. Nevertheless, there is the intuition that only one of these two inequalities is really the more stringent requirement, and thus the one that is necessary to satisfy at any given combination of Ω and U. The introduction of the parameter α, a proportion between the norms of the two multiplicative noise sources, allowed the requirement of satisfying only one inequality at a time to become clearer. Against intuition the necessary bound resulted to be independent of U. In summary the conditions, in light of Proposition 2, are

$$\begin{cases} \|\boldsymbol{\Theta}\|_s^2 < \dfrac{1}{U}\sqrt{\dfrac{2-\Omega}{\alpha\Omega}} & if \;\; \dfrac{1}{\sqrt{\alpha}} + \sqrt{\alpha} < 2\sqrt{\dfrac{2-\Omega}{\Omega}} \\ \|\boldsymbol{\Theta}\|_s^2 < \dfrac{1}{U}\dfrac{2(2-\Omega)}{(1+\alpha)\Omega} & if \;\; \dfrac{1}{\sqrt{\alpha}} + \sqrt{\alpha} > 2\sqrt{\dfrac{2-\Omega}{\Omega}} \end{cases} \quad (30)$$

6. SIMULATION EVALUATION

In this section, the closed-loop power allocation scheme studied for the uplink is evaluated through numerical simulations of a multiple-access wireless network. The parameters of the simulation are illustrated in Table 1, where all the implementations were carried out in Matlab. A code-division multiple-access technology was considered at each BS, where m-sequence codes were employed for spreading the information in time-domain (Proakis and Salehi, 2007). For each MU, its channel gain energy was modelled by two components: slow and fast-scale variations (Gunnarsson and Gustafsson, 2003), i.e.

$$|h_{i,l}[k]|^2 = \underbrace{(Y[k])^{-1}\left(\frac{0.1}{d_{i,l}[k]}\right)^{\alpha}}_{slow-scale} \underbrace{g[k]}_{fast-scale} \quad \forall i, l \in \mathcal{I} \quad (31)$$

where $Y[k]$ is a log-normal random variable, $d_{i,l}[k]$ denotes the distance of i-th MU with respect to the BS assigned to l-th MU at k-time instant, and $g[k]$ is a random variable with a Rayleigh distribution and unitary mean ($\mathcal{E}\{g[k]\} = 1$). In our simulations, the slow-scale components were updated every $K = 20$ samples, meanwhile, the fast-scale components at each sampling interval. All the MUs followed a random-walk displacement profile in the spatial plane. This profile is characterized by two coordinates $(\rho_{i,x}[k], \rho_{i,y}[k])$ for i-th MU that are updated according to the next stochastic model

Table 1. Parameters of the Wireless Network during the Simulation Evaluation.

Physical Parameter	Variable	Value
Processing gain	N	32
Noise variance	ν^2	−90 dBm
Minimum transmission power	p_{min}	1 pW
Maximum transmission power	p_{max}	500 mW
Control Gain	Ω	0.05
Roundtrip delay	n_{RT}	2

$$\rho_{i,x}[k+1] = \rho_{i,x}[k] + \theta\nu_{i,x}[k]$$
$$\rho_{i,y}[k+1] = \rho_{i,y}[k] + \theta\nu_{i,y}[k] \quad (32)$$

where $\nu_{i,x}[k]$ and $\nu_{i,y}[k]$ are zero-mean and unitary variance random variables with a Gaussian distribution. The constant θ is chosen such that the mean velocity of the profile is v_o (km/h) $\Rightarrow \theta = (v_o/3.6T_sK)\sqrt{2/\pi}$, where $T_s = 1/1500$ s is the update time for power allocation in the wireless network. Consequently, if (x_m, y_m) denotes the spatial location of the m-th BS assigned to l-th MU, the distance $d_{i,l}[k]$ is calculated by

$$d_{i,l}[k] = \sqrt{(x_m - \rho_{i,x}[k])^2 + (y_m - \rho_{i,y}[k])^2} \quad \forall i \in \mathcal{I}. \quad (33)$$

Now, for the i-th MU, a spreading code $\mathbf{c}_i \in \mathbb{R}^N$ is assigned before data transmission. In this work, we assumed that there is spreading code reuse among all BSs, in order to have a challenging scenario. Moreover, at the detection process of each BS, there is a correlating sequence $\boldsymbol{\xi}_i \in \mathbb{R}^N$, according to a linear detection strategy: matched filter, zero-forcing, minimum mean-square error (MMSE) or serial interference canceller (Proakis and Salehi, 2007). In this framework, the data energy, interference and noise parameters $(\delta_{ii}[k], \delta_{il}[k], \omega_i[k])$ after linear detection are given by $\delta_{i,i}[k] = |h_{i,i}[k]|^2(\boldsymbol{\xi}_i^\top \mathbf{c}_i)^2$, $\delta_{i,l}[k] = |h_{i,l}[k]|^2(\boldsymbol{\xi}_i^\top \mathbf{c}_l)^2$, and $\omega_i[k] = \nu^2(\mathbf{c}_i^\top \mathbf{c}_i)^2$. During the simulations, the MMSE detector was implemented at each BS (Campos-Delgado and Luna-Rivera, 2013-A).

Without loss of generality, the objective SINR will be considered the same for all MUs in our evaluations, i.e. $\gamma_i^{obj} = \gamma^{obj}$ for all $i \in \mathcal{I}$. In each BS, the number of MUs is half of the processing gain, i.e. there are 16 MUs per BS. The LQG controller in (16) was considered with parameter $\Omega = 0.05$ in the closed-loop power allocation scheme. First, a Monte Carlo evaluation was carried out by varying the number of active BSs in the wireless network at $\gamma^{obj} = 8$ dB with 5,000 closed-loop simulations of 100 time iterations, where in each one, the channel realizations in (31) are randomly generated. In this way, the number of MUs in the wireless network was increased from 32 (2 BSs) to 64 (4 BSs), and as a consequence, the interference which is measured by $\|\boldsymbol{\Theta}\|_s^2$ raises constantly. For each closed-loop simulation, $\|\boldsymbol{\Theta}\|_s^2$ was computed numerically by (13), in the meantime $\|\boldsymbol{\Xi}\|_s^2 = 0.1$ was kept constant in our evaluation. With this information at hand, the upper bounds on the MUs in the wireless network were calculated through (17) and (18). Note that in this case $2\sqrt{(2-\Omega)/\Omega} = 12.49$, so it is argued that the first inequality in (30) or equivalently (17) will be the more restrictive. Also, the mean power and measured SINR per MU were computed. The overall results of the Monte Carlo simulation are described in Table 2. This table illustrates that as the number of BSs increases, this tendency is followed by the interference $\|\boldsymbol{\Theta}\|_s^2$ and the mean transmission power per MU. Hence as more BSs incorporate into the network, the maximum number of MUs allowable is reduced. In this case, the inequality in (17) is, as expected, the more stringent requirement. Finally, the power allocation scheme by the LQG controller in (16) is able to manage efficiently the induced interference and achieve the objective SINR in all cases (see last column in Table 2).

Table 2. Monte Carlo Evaluation for Different Number of BSs in the Wireless Network ($\gamma^{obj} = 8$ dB).

BSs	$\|\boldsymbol{\Theta}\|_s^2$	Max U by (17)	Max U by (18)	Mean Power per MU (W)	Mean SINR per MU (dB)
2	0.0027	1199.17	6135.43	0.0124	8.02
3	0.3894	100.17	195.76	0.0132	8.02
4	0.6756	76.00	113.86	0.0175	8.02

Table 3. Monte Carlo Evaluation for Different Objective SINRs in the Wireless Network (BS=3).

γ^{obj}	$\|\boldsymbol{\Theta}\|_s^2$	Max U by (17)	Max U by (18)	Mean Power per MU (W)	Mean SINR per MU (dB)
7	0.2556	123.58	294.03	0.0111	7.02
8	0.3894	100.17	195.76	0.0132	8.02
9	0.4760	90.60	160.90	0.0195	9.03

A new Monte Carlo evaluation was considered with also 5,000 closed-loop simulations and 100 time-iterations in each one. However, in this new condition, the objective SINR γ^{obj} was varied in the network among 7, 8 and 9 dB with BS=3. The results of this evaluation are presented in Table 3. As expected, the interference $\|\boldsymbol{\Theta}\|_s^2$ and the mean transmission power per MU increase if γ^{obj} is raised, due to linear dependence of $\|\boldsymbol{\Theta}\|_s^2$ in (6) on this parameter. Once more, the inequality in (17) is the more stringent requirement for the maximum number of MUs. Also, the LQG power allocation in (16) was capable to reaching in average the objective SINRs (see last column in Table 3).

Finally, in order to visualize the time response with 4 BSs and $\gamma^{obj} = 8$ dB, Fig. 3 illustrates the initial spatial location of the BSs and MUs in the simulation, and Fig. 4 presents the time responses of the resulting transmission power and measured SINR per each MU, as well as their mean traces. In this scenario, the MUs located closer to the BS will require less transmission power than the ones located farther away in order to achieve the objective SINR. Also, the SINR traces show the effect of the slow and fast-scale channel variations described in (31), since the slow-scale variations every 20 iterations generate abrupt transitions in the SINR, and the fast-scale changes produce a consistent error around the setpoint of 8 dB. Nonetheless, in average, all the MUs achieve the objective SINR despite the multiple-access environment and multiplicative noise.

7. CONCLUSIONS

In this paper, we extended our analysis of power allocation in wireless networks, and validated it through numerical simulations. By establishing a numerical relation between the size of the interference $\|\boldsymbol{\Theta}\|_s^2$ and the multiplicative

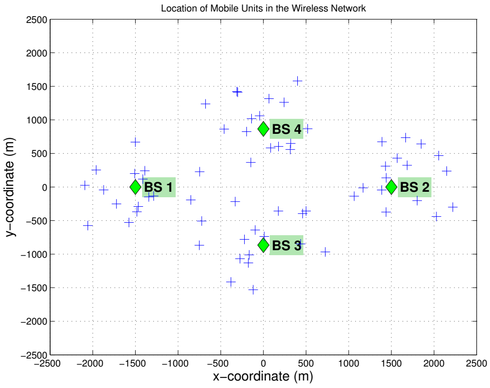

Fig. 3. Initial Random Location of MUs for 4 BSs.

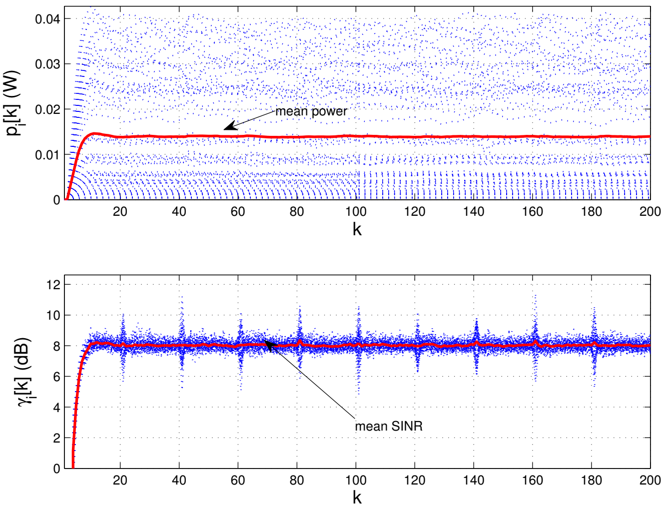

Fig. 4. Performance of Power Allocation Scheme for 4 BSs.

noise $\|\Xi\|_s^2$, we were able to define a unique stability bound for power allocation in a closed-loop structure. Moreover, a numerical evaluation was carried out in a wireless network with multiple BSs and variable number of MUs. In the simulation scenario, slow and fast-scale variations were considered in the channel model, as well as a random displacement time-profile of the MUs. Hence, the induced interference in the network is the limiting factor for closed-loop operation, where the power allocation scheme was able to achieve the desired QoS despite the multiple-access interference and multiplicative noise component.

REFERENCES

J. Proakis and M. Salehi. *Digital Communications*. Mc. Graw-Hill, 5th Ed., 2007.

K. Fazel and S. Kaiser. *Multi-Carrier and Spread Spectrum Systems: From OFDM and MC-CDMA to LTE and WiMAX*, 2nd Edition, John Wiley & Sons, 2008.

D. U. Campos-Delgado and Martin Luna-Rivera. Optimal Pre-equalization for Wireless MC-CDMA Systems under QoS Requirements. *IET Comm.* 7(14):1497–1509, 2013.

T. Alpcan, X. Fan, T. Basar, M. Arcak, and J.T. Wen. Power control for multicell CDMA wireless networks: A team optimization approach'. *Wireless Networks* 14(5):647–657, 2008.

F. Gunnarsson, and F. Gustafsson. Control theory aspects of control in UMTS. *Control Eng. Practice* 11:1113–1125, 2003.

S. Koskie and Z. Gajic. Signal-to-interference-based power Control for wireless networks: a survey, 1992–2005. *Dynamics of Continuous, Discrete and Impulsive Systems B: Applications and Algorithms* 13(2):187–220, 2006.

C.U. Saraydar, N.B. Mandayam, and D.J. Goodman. Efficient Power Control Via Pricing in Wireless Data Networks. *IEEE Trans. on Commun.* 50(2):291–303, 2002.

D.U. Campos-Delgado, J. M. Luna-Rivera and F.J. Martinez-Lopez. Distributed Power Control Algorithms in the Uplink of Wireless CDMA Systems. *IET Control Theory & Appl.* 4(5): 795-805, 2010.

N. Zhao, Z. Wu, Y. Zhao, and T. Quan, Robust H_∞ Power Control for CDMA Systems in User-Centric and Network-Centric Manners. *ETRI Journal* 32(4):399–407, 2009.

M.G. Safonov, A. Paul, M. Akar and U. Mitra. Adaptive Power Control for Wireless Networks using Multiple Controllers and Switching. *IEEE Trans. Neural Netw.* 16(5):1212–1218, 2005.

G.J. Foschini and Z. Miljanic. A Simple Distributed Autonomous Power Control Algorithm and its Convergence, *IEEE Trans. on Vehic. Tech.* 42(4):641-646, 1993.

F. Gunnarsson and F. Gustafsson. Dynamical effects of time delays and time compensation in power controlled DS-CDMA. *IEEE J. Sel. Areas Commun.* 19:141–151, 2001.

G. G. Messier, J. A. Hartwell, and R. J. Davies. A Sensor Network Cross-Layer Power Control Algorithm that Incorporates Multiple-Access Interference. *IEEE Trans. on Wireless Commun.* 7(8):2877–2883, 2008.

S. Lee. *Spread Spectrum Cdma: Is-95 and Is-2000 for RF Communications.* Ed. Mc. Graw-Hill, 2002.

W. Su, T. Qi, J. Chen and M. Fu. Optimal Tracking Design of an MIMO Linear System with Quantization Effects. *Proc. of the 18th World Congress IFAC*, Milano, Italy, August 28 - September 2, 2011.

M. Fu and L. Xie. The Sector Bound Approach to Quantized Feedback Control. *IEEE Trans. on Automatic Control* 50(11):1698-1711, 2005.

D.U. Campos-Delgado and J.M. Luna-Rivera. Distributed Power Allocation Algorithm in Wireless Networks under SNR Constraints. *AEU - International Journal of Electronics and Communications* 67(12):1015–1024, 2013.

D.E. Quevedo and T. Wigren. Design of Embedded Filters for Inner-Loop Power Control in Wireless CDMA Communication Systems. *Asian J. of Control* 14(4): 891–900, 2012.

J. Lu and R.E. Skelton. Robust Variance Control for Systems With Finite Signal-to-Noise Uncertainty. *Automatica*, 36:511-525, 2000.

J. Lu and R.E. Skelton. Mean-square Small Gain Theorem for Stochastic Control: Discrete-Time Case. *IEEE Trans. on Automatic Control* 47(3):490–494, 2002.

D.U. Campos-Delgado, J. M. Luna-Rivera and A.J. Rojas. Analysis of Distributed Power Allocation in Wireless Networks under Multiplicative Noise and Interference Uncertainty. *2014 American Control Conference.* Portland, Oregon, June 3-6, 2014.